

## Article

# Heparin in Acid and Alkaline Environments—A Study of the Correlations between Hydrodynamic Properties and Desulphation

Aleksandra Maria Kozłowski<sup>1,\*</sup>, Vlad Dinu<sup>2</sup>, Thomas MacCalman<sup>2</sup>, Alan Mark Smith<sup>1</sup>, Johannes Peter Roubroeks<sup>3</sup>, Edwin Alexander Yates<sup>4</sup>, Stephen Ernest Harding<sup>2</sup> and Gordon Alistair Morris<sup>1,\*</sup>

<sup>1</sup> Biopolymer Research Centre, School of Applied Sciences, University of Huddersfield, Huddersfield HD1 3DH, UK

<sup>2</sup> National Centre for Macromolecular Hydrodynamics, School of Biosciences, University of Nottingham, Sutton Bonington Campus, Leicestershire LE12 5RD, UK

<sup>3</sup> LEO Pharma A/S, Industriparken 55, 2750 Ballerup, Denmark

<sup>4</sup> Department of Biochemistry and Systems Biology, Institute of Systems, Molecular and Integrative Biology, University of Liverpool, Liverpool L69 7ZB, UK

\* Correspondence: aleksandra.kozłowski@chalmers.se (A.M.K.); g.morris@hud.ac.uk (G.A.M.)

**Abstract:** This work evaluated the hydrodynamic properties of heparin hydrolysed at temperatures ranging from 40 °C to 80 °C in buffered acid and alkaline environments. The correlation between hydrodynamic parameters led to the conclusion that polymer conformational changes appeared to be minimal until chain depolymerisation, initiated at pH 1 and 80 °C. However, the synergy of conformational changes, even if minimal, and sulphate loss observed at pH 1, pH 3 and pH 12 (various temperatures) resulted in a loss of the antifactor Xa activity. Therefore, the ‘contribution’ of conformational changes should be added to the generally recognized effect of desulphation towards the activity of heparin. This is of significance as the processing of medical heparin is complex, and requires adjustment of several physical and chemical factors, including pH and temperature.

**Keywords:** heparin desulphation; hydrodynamic properties; activity



**Citation:** Kozłowski, A.M.; Dinu, V.; MacCalman, T.; Smith, A.M.; Roubroeks, J.P.; Yates, E.A.; Harding, S.E.; Morris, G.A. Heparin in Acid and Alkaline Environments—A Study of the Correlations between Hydrodynamic Properties and Desulphation. *Polysaccharides* **2023**, *4*, 88–98. <https://doi.org/10.3390/polysaccharides4020007>

Academic Editor: Emiliano Bedini

Received: 7 March 2023

Revised: 20 March 2023

Accepted: 22 March 2023

Published: 23 March 2023



**Copyright:** © 2023 by the authors. Licensee MDPI, Basel, Switzerland. This article is an open access article distributed under the terms and conditions of the Creative Commons Attribution (CC BY) license (<https://creativecommons.org/licenses/by/4.0/>).

## 1. Introduction

At a first glance, heparin could be perceived as a simple molecule. It is composed of alternating monomeric units of uronic acid, i.e.,  $\alpha$ -L-iduronate (IdoA) or  $\beta$ -D-glucuronate (GlcA) and  $\alpha$ -D-glucosamine (GlcN), connected by 1–4 links to form a linear, unbranched structure [1–3]. The initial polysaccharide, consisting of a  $[\text{GlcA-(1,4)-GlcNAc}]_n$  polymer, is successively modified by 12 biosynthetic enzymes. The actions of N-deacetylase/N-sulfotransferase (NDST), C-5 epimerase (C5 epi) and O-sulfotransferases (OSTs) result in the production of highly sulphated, uronic-acid-rich heparin chains [3–6]. Each disaccharide residue has several potential sulphation sites at position 2- (2S-) in IdoA and positions 6-, 3- and 2- (6S-, 3S- and NS-, respectively) in GlcN, providing, in principle, 32 possible structural modifications to each disaccharide building block; however, it is not completely understood how these modifications are regulated [6–8]. The result is a complex substitution pattern along the heparin chains of various lengths, which deprives heparin of ‘the simple molecule’ status.

In heparins, particularly in the commercial ones, the average degree of sulphation equals  $\sim 2.7$  per disaccharide unit; it equates to around 97 sulfo-groups per heparin polymer chain of molecular weight  $2 \times 10^4$  g/mol [7,9,10]. The overall negative charge density is additionally increased by the carboxyl groups on the uronic-acid residues, making heparin one of the most negatively charged biological macromolecules [3,11]. A major

contribution to the biological activity of heparin results from electrostatic interactions between these negatively charged (especially sulpho) groups with basic amino-acid residues (arginine, lysine and, at appropriate pH values, also histidine) of heparin-binding proteins [4,8,12]. The selectivity of binding controls numerous important biological processes, among which the ability of heparin to influence the coagulation of blood, i.e., the anticoagulant activity, has been investigated with the greatest attention [2,13,14]. It has been shown that changes in the sulphation pattern of heparin affect its biochemical activity; for example, 2/6-O-desulphated heparin demonstrated antifibrotic and anti-inflammatory properties [15–17], and the removal of N- and 3-O-sulphate reduced the anticoagulant activity of heparin [8,16,18].

In the early work on heparin conformation, the aqueous form of the macromolecule was proposed to have an extended, helical structure [19,20]. The major sources of the flexibility of such structured polysaccharides are the torsion angles of the glycosidic bonds,  $\Phi$  and  $\Psi$ , located between the monosaccharide residues [21–23] and the propensity of the IdoA2S to exist in several conformations [24]. However, the studies on the heparin structure in solution clarified that the unique flexibility of its chain arises from the combined effect of multiple factors, for example; ionic concentration of counter cations [7,8,20], hydrogen bonding [25], iduronate dynamics [26], the degree and pattern of sulphation [1,27,28] and chain length [29–31], summarised in Figure 1.

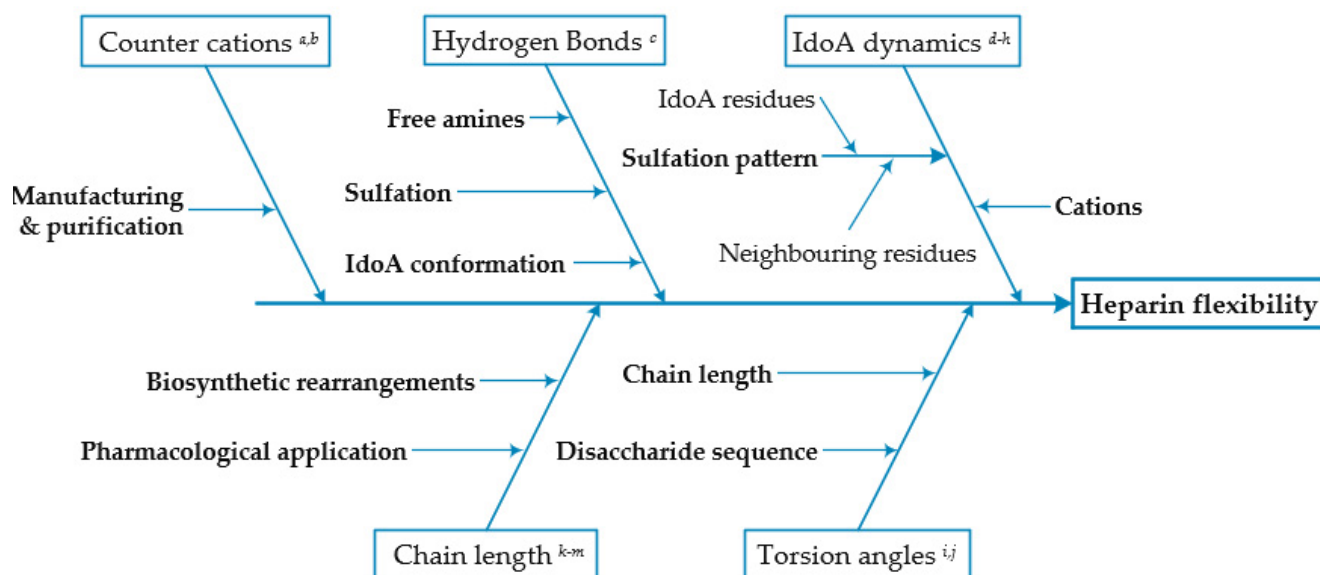


**Figure 1.** The cause-and-effect diagram assesses the effect of several interlinked variables on the flexibility of the heparin chain. Based on: [7,8] <sup>a,b</sup>, [25] <sup>c</sup>, [1,26–28] <sup>d–h</sup>, [6,32] <sup>i,j</sup> and [29–31] <sup>k–m</sup>.

While heparin has been reported to interact with hundreds of other proteins [33], in most cases, little or no information about their structure–activity relationships is available. The structural manipulations have clear consequences for the pharmacological activity of heparin. This, in turn, has created an opportunity to diversify the therapeutic profile of heparin. It has also underlined the necessity to cautiously examine heparin preparations, to avoid undesired pharmacological effects, such as changes in substitution pattern, depolymerisation or changes to global hydrodynamic properties which may occur to heparin during the production process or through inadvertent exposure to extreme conditions of temperature or pH.

For sulphated polysaccharides such as heparin there is a serious risk of hydrolytic sulphate loss, especially when operating at the extremum of the pH scale [9,23,34,35]. Owing to desulphation, the intramolecular electrostatic repulsion forces between the molecules of polysaccharides decrease, allowing more flexible and less extended conformation [36]. The heparin with the lowered degree of sulphation might be expected to behave as a more

compact molecule when in solution, compared to a molecule of unchanged sulphation pattern and identical degree of polymerisation. Taking another look at the diagram presented in Figure 1, it could be concluded that any change to the distribution of negatively charged groups has the potential to alter the conformation of heparin, ergo, affect its pharmacological functionality and/or off-target activity.

The environment that heparin is normally found in (as a finished pharmacological product) and processed in (as raw material), i.e., aqueous medium, provides plenty of opportunities for hydrolytic desulphation. Furthermore, both the storage of heparin drug and the multistage manufacturing process require many factors (i.e., temperature, chemicals, time, pressure, etc.) to be adjusted for the sake of optimal conditions. For example, the temperature can be as low as 4 °C during precipitation, increasing to 60 °C for alkalase digestion, and being further elevated to ~80 °C during the isolation and drying of heparin [37]. Then, the analysis of pharmacologically active unfractionated heparin and its digestion into low-molecular-weight products requires heat application from 40 °C to 80 °C [29,37,38]. The pH changes usually apply to the treatment of raw material (i.e., pig mucous) during heparin extraction and the depolymerisation of unfractionated products; these vary between pH 1 and pH 12, depending on the treatment stage [37–39].

It has been demonstrated that variations in temperature and pH effectively alter the degree of sulphate substitution and cause structural changes along the heparin chain in aqueous solutions [9,34,35,40–44]. In these studies, the scientific questions were mostly asked from the perspective of molecule stability, including our contribution to the discussion on the scope of hydrolytic desulphation and conformation of heparin in buffered alkaline and acidic media [34,40]. Here, we discuss the effect of desulphation and depolymerisation observed in conditions corresponding to heparin storage and manufacturing conditions, i.e., pH range from 1 to 12 (chosen examples) and temperature from 40 °C to 80 °C (chosen examples), towards the physical properties (i.e., size and conformation) and their effect on the pharmacological performance of heparin. For this purpose, advanced hydrodynamic methods were employed. The conclusions concerning the conformation and molecular expansion of heparin that has been hydrolysed in a range of buffered aqueous solutions and a set of temperatures are based on the results of the sedimentation velocity in analytical ultracentrifugation; the weight-average molecular weight  $M_w$ , polydispersity and intrinsic viscosity are confirmed with size-exclusion chromatography coupled to a series of detectors. The collected results are considered together with the pharmacological activity and confirm the relation between the sulphation degree, physical properties and therapeutic functionality of heparin.

## 2. Materials and Methods

### 2.1. Materials

All reagents used in this study were of analytical grade or higher. All solutions were prepared in Milli-Q ultrapure water of  $\geq 18.2$  M $\Omega$ ·cm resistivities at 25 °C. Heparin sodium salt (porcine mucosal;  $M_{w,0} \approx 20,000$  g/mol,  $M_w/M_n = 1.1$ ) was provided by LEO Pharma (LEO Pharma A/S, Cork, Ireland/Ballerup, Denmark) and used without further purification. Chemicals used for buffering systems, i.e., potassium chloride, sodium citrate, citric acid and dibasic sodium phosphate, were purchased from Sigma-Aldrich (Sigma-Aldrich, Dorset, UK), while concentrated hydrochloric acid (12.1 M), sodium hydroxide (pearls) and disodium tetraborate decahydrate were purchased from Fisher Scientific (Fisher Scientific, Loughborough, UK).

### 2.2. Analytical Solutions

Heparin stock: The aqueous stock of final concentration 10 mg/mL was prepared by dissolving 10 g of oven-dried (48 h/60 °C) heparin in 1 L of water with stirring for 12 h.

Buffered heparin solutions: Buffering systems (0.1 M) that ranged between pH 1 and 12 were prepared in sealable glass bottles (250 mL) by dissolving the appropriate mass of buffering salts directly in heparin stock at room temperature with vigorous stirring until

fully dissolved. This approach allowed full control over the concentration and volume of the hydrolysed samples, and only minimal (if any) pH adjustment. The composition details of buffering systems are summarized in Table 1.

**Table 1.** Details of buffering systems applied in heparin hydrolysis protocol.

Buffering System	Formula	pH Range
Hydrochloric Acid— Potassium Chloride [45]	HCl + KCl	1.0–2.2
Citrate Buffer [45]	$C_6H_5O_7H_2 + C_6H_5O_7Na_2 \cdot 2H_2O$	3.0–6.2
Borax Buffer [46]	$Na_2B_4O_7 \cdot 10H_2O + NaOH$	9.2–10.8
Phosphate Buffer [46]	$NaH_2PO_4 + NaOH$	10.9–12.0

### 2.3. Heparin Hydrolysis

Detailed protocols of acidic and alkaline hydrolysis of heparin have been described in our earlier publications on heparin stability [34,40]. In brief, heparin (sodium form) was thermally stressed over time at various pHs (see Table 1). Samples buffered at the pH range from 1 to 12 were prepared in separate, sealable glass bottles (250 mL). The bottles were incubated in a water bath at 40 °C, 60 °C or 80 °C for 48 h. Samples were immediately cooled down in an ice bath and neutralised with 1.0 M NaOH or 1.0 M HCl to pH 7.0–7.5. The neutralised hydrolysates were further diluted with deionised water to a final concentration of 5 mg/mL (5000 ppm).

### 2.4. Analytical Methods

The analytical data were recorded with original software matching individual techniques (details given in methodology). The numerical results were extracted and replotted (where applicable) in OriginPro v. 2020 (OriginLab Corporation, Northampton, MA, USA).

#### 2.4.1. Size-Exclusion Chromatography

Weight-average molecular weight ( $M_w$ ) of hydrolysed samples was measured with the size-exclusion chromatography (SEC) coupled with multiangle light scattering (MALS; DAWN+) and refractive index (RI; Optilab T-REX) detectors (Wyatt Technology Corporation, Santa Barbara, USA). Samples were separated on TSK G4000 SW<sub>XL</sub> and TSK G3000 SW<sub>XL</sub> columns (Tosoh Bioscience, Tokyo, Japan), protected by a similarly packed guard column. The flow of the 0.1 M NH<sub>4</sub>OAc + 0.05% (*w/v*) NaN<sub>3</sub> mobile phase was set to 0.6 mL/min at 30 °C. The concentrations of analysed samples were 5 mg/mL (5000 ppm). The monodisperse bovine serum albumin (BSA) was prepared at a concentration of 2 mg/mL (2000 ppm) and used as the system normalisation standard, prepared in buffers identical to those of experimental samples (see Table 1). Each sample was filtered through a 0.45 µm regenerated-cellulose (RC) syringe filter (17 mm, Thermo Fisher Scientific, Paisley, UK). Data were analysed using Astra software v. 6.1.5 (Wyatt Technology Corporation, Santa Barbara, CA, USA). Refractive index increments ( $dn/dc$ ) of 0.131 mL/g and 0.185 mL/g were used, respectively, for heparin and BSA [47,48]. For intrinsic viscosity determination, the experimental procedure was repeated on a similar SEC set-up (LB-G 6B guard column and LB-805 column (Shodex™) connected in series) with an additional online Wyatt Viscostar-II (Wyatt Technology, Santa Barbara, CA, USA) differential-pressure-viscosity (DPV) detector at the National Centre for Macromolecular Hydrodynamics (NCMH), University of Nottingham.

#### 2.4.2. Sedimentation Velocity in the Analytical Ultracentrifuge

The change in sedimentation velocity was measured using an Optima XLI Analytical Ultracentrifuge (Beckman Instruments, Palo Alto, CA, USA). Before the analytical procedure, the selected heparin hydrolysates (2.5 mL) were loaded onto the PD-10 column, prepacked with Sephadex™ G-25 Medium (GE Healthcare Life Sciences, Little Chalfont,

UK) and desalted with water. The eluates were freeze-dried, accurately weighed and redissolved in 0.2 M acetate buffer (pH 4.3) to a final concentration of 1.0 mg/mL (1000 ppm) and left overnight (with stirring). Samples and the appropriate buffer (see Table 1) were loaded into the solution and reference channels, respectively of a double sector 12 mm optical path length cell and centrifuged at 50,000 rpm at 20.0 °C. The movement of the sedimenting boundary in the analytical cell was recorded with the Rayleigh interference optical system and converted to concentration (in units of fringe displacement relative to the meniscus,  $j$ ) versus radial position,  $r$  [49]. The data were analysed using the “least squares,  $c(s)$  model” available in SEDFIT (Version 9.4b) software [50–52].

#### 2.4.3. Pharmacological Activity Assay

The changes in the pharmacological activity of hydrolysed samples were disclosed by the courtesy of LEO Pharma (LEO Pharma A/S, Ballerup, Denmark). Samples were analysed (in duplicate) against the heparin-sodium standard using the Pentra Haematology Analyzer (HORIBA, Ltd., Kyoto, Japan), following the industrial antifactor Xa protocol.

### 3. Results and Discussion

The choice in samples presented in this study includes those with varied extents of desulphation following treatment in acidic and alkaline environments, discussed in previous studies on heparin stability [34,40,53]. Consequently, the samples that lost very little or no sulphate, i.e., pH 6/48 h/40 °C, pH 10/48 h/40 °C and pH 11/48 h/60 °C; a sample with moderate sulphate loss, i.e., pH 3/48 h/60 °C, and the samples with significant sulphate loss, i.e., pH 12/48 h/80 °C and pH 1/48 h/80 °C, were analysed, as summarised in Table 2.

**Table 2.** Degree of desulphation for heparin samples analysed in the presented study.

Sample	Sulphate Removed (%)	Reference
Heparin Standard	<LOQ <sup>*,1</sup>	[53]
pH 6/48 h/40 °C	<LOQ *	[34]
pH 10/48 h/40 °C	<LOQ *	[40]
pH 3/48 h/60 °C	5.4 (0.8)	[34]
pH 11/48 h/60 °C	<LOQ *	[40]
pH 12/48 h/80 °C	14.5 (1.4)	[40]
pH 1/48 h/80 °C	59.8 (1.6)	[34]

\* (<Limit of Quantification ~0.001%), <sup>1</sup> free sulphate measured in heparin standard.

#### 3.1. Analysis with Size-Exclusion Chromatography

The results of the SEC-MALS-RI analysis are summarised in Table 3. The weight-average molecular weight ( $M_w$ ) decreased with the severity of the applied conditions (Figure 2) [17,28]. The loss of  $M_w$  did not affect their polydispersity ( $M_w/M_n$ ) (results not shown), apart from at pH 1 when minor glycosidic scission was observed [34]. The decrease in  $M_w$  was consistent with the changes in intrinsic viscosity ( $[\eta]$ ), which indicates minor conformational changes, except at pH 1 (due to depolymerisation [34]) and pH 12 (due to deacetylation [40]). This relation suggests that minor to moderate sulphate loss does not affect the shape of heparin in solution to the same degree as chain degradation.

**Table 3.** Summary of measured parameters of hydrolysed heparin, concerning applied pH and temperature.

Sample	$M_w$ (g/mol)	$[\eta]_w$ (mL/g)	$s_{20,w}$ (S)	$D_{20,w}$ $10^7$ ( $\text{cm}^2\text{s}^{-1}$ )	$R_h$ (nm)	$f/f_0$ [ $\eta$ ]	$L_p$ (nm)	$M_L$ (g/mol.nm)	$L_p/M_L$ (mol.nm <sup>2</sup> /g)	$a$	AntiX <sub>a</sub> <sup>1</sup> (IU/mL)
Heparin Standard	20,000 (700) <sup>a</sup>	25.7 (0.1) <sup>a</sup>	1.71 (0.05)	4.37 (0.56)	4.62 (0.28)	2.8	6	559 (1) <sup>a</sup>	0.0107	1.02	911 (10) <sup>a</sup>
pH 6/48 h/40 °C	19,900 (500) <sup>a</sup>	26.3 (0.1) <sup>a</sup>	1.86 (0.05)	4.54 (0.37)	4.54 (0.18)	2.9	6	559 (1) <sup>a</sup>	0.0107	1.02	509 (5) <sup>d</sup>
pH 10/48 h/40 °C	19,800 (600) <sup>a</sup>	25.0 (0.1) <sup>a</sup>	1.86 (0.05)	4.59 (0.40)	4.48 (0.19)	2.8	5	559 (1) <sup>a</sup>	0.0089	0.95	723 (8) <sup>b</sup>
pH 3/48 h/60 °C	17,900 (1300) <sup>a</sup>	26.4 (0.2) <sup>a</sup>	1.79 (0.05)	4.77 (0.31)	4.36 (0.14)	2.9	6	548 (2) <sup>b</sup>	0.0109	1.03	266 (6) <sup>f</sup>
pH 11/48 h/60 °C	17,400 (900) <sup>a</sup>	24.3 (0.3) <sup>a,b</sup>	1.70 (0.05)	4.81 (0.46)	4.26 (0.19)	2.7	6	559 (1) <sup>a</sup>	0.0107	1.04	682 (1) <sup>c</sup>
pH 12/48 h/80 °C	15,100 (700) <sup>a,b</sup>	22.3 (0.3) <sup>b</sup>	1.70 (0.05)	5.34 (0.34)	3.89 (0.12)	2.7	6	529 (3) <sup>c</sup>	0.0113	1.04	322 (1) <sup>e</sup>
pH 1/48 h/80 °C	14,600 (1900) <sup>b</sup>	13.2 (0.3) <sup>c</sup>	1.83 (0.05)	6.22 (0.63)	3.29 (0.16)	2.3	2	437 (3) <sup>d</sup>	0.0046	0.50	<1 <sup>g</sup>
Pavlov et al. [54]	4000–37,000	8.0–40	1.30–3.18	3.95–15.40	1.39–5.42	1.6–3.0	3–6	570 (50)	0.0061–0.0105	0.90 (0.06)	n/a

Numbers in brackets stand for the statistical consistency of the data calculated by ASTRA and SEDFIT algorithms. The means of each property followed by different letters in the same column are significantly different ( $p \leq 0.05$ ).  $D_{20,w}$  and  $R_h$  were estimated using the Svedberg and Stokes–Einstein equations, respectively (see for example ref. [52]).  $a$ —the intrinsic viscosity exponent; <sup>1</sup> Antifactor Xa activity.

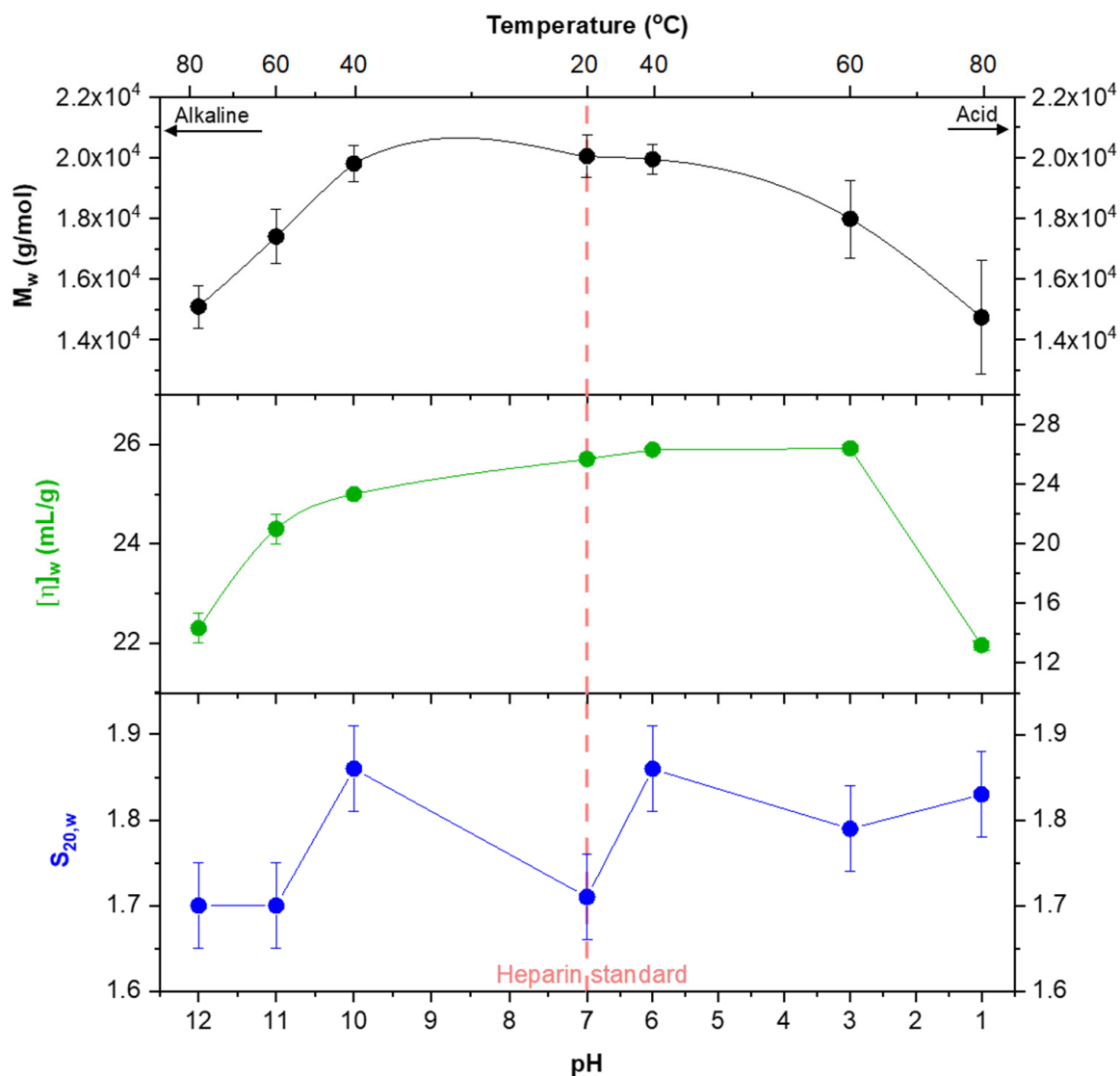


**Figure 2.** Weight-average molecular weight ( $M_w$ ), intrinsic viscosity ( $[\eta]$ ) and sedimentation coefficient ( $s_{20,w}$ ) for heparin samples, plotted against hydrolytic pH and temperature. The error bars indicate the statistical consistency of the data calculated by ASTRA and SEDFIT algorithms; where not visible (i.e., acid scale  $\eta_w$ ), the bars are concealed by data points.

### 3.2. Results of Analytical Ultracentrifugation

The sedimentation coefficient,  $s_{20,w}$ , showed a similar trend to changes observed in  $M_w$  and  $[\eta]$ , as presented in Figure 2. Compact molecules have less friction, and therefore sediment more quickly with less resistance to the flow, hence, they show reduced viscosity [36,49,55]. Previous studies have shown that considerable changes in these hydrodynamic parameters followed definite depolymerisation of the macromolecular chain [54]. Referring to the depolymerisation of heparin described in Section 3.1, it could be assumed that the level of chain scission was insufficient (in most cases minimal or not observed) to affect the molecular conformation of heparin to a significant degree, except at pH 1 [34]. A similar conclusion can be drawn when looking at the desulphation, and in the case of pH 12, accompanying deacetylation (refs. [34] and [40]). The diffusion coefficient ( $D_{20,w}$ ), a measure of the mass of the dissolved material transported per unit of time [21,23], increased proportionally to  $M_w$  loss, as expected (Table 3). The hydrodynamic radius ( $R_h$ ), which relates to the apparent volume of molecules in the solution [22,56], decreased with the  $M_w$  and sulphate loss (Table 3).

### 3.3. Conformational Analyses

#### 3.3.1. Mark–Houwink–Kuhn–Sakurada (MHKS) Relations

For a homologous series of polymers of different molecular weights, the chain conformation can be estimated from the molecular-weight dependency of the intrinsic viscosity ( $[\eta]$ ), following Equation (1) [57].

$$[\eta] = \kappa_{\eta} M^a \quad (1)$$

where  $\kappa_{\eta}$  and  $a$  are obtained from the intercept and slope of the double log plot of  $[\eta]$  vs.  $M$  from size exclusion coupled online with light-scattering (LS) and differential-pressure-viscosity (DPV) detectors. The value of  $a$  can be used as an estimation of gross macromolecular conformation and, hence, an  $a$  value of  $\sim 0$  corresponds to spheres, 0.5–0.8 to random coils, and up to 1.8 to rigid rods [57]. Therefore, all conditions other than pH 1 result in a heparin structure with an  $a$  exponent of  $1.02 \pm 0.03$ , which is consistent with a rigid structure (Table 3). The removal of  $\sim 60\%$  of the sulphate groups at pH 1 and the corresponding loss of negative charge on the polymer chain results in a reduction in chain stiffness and a random coil conformation ( $a = 0.50$ ) for this partially desulphated heparin.

#### 3.3.2. Translational Frictional Ratio

The translational frictional ratio,  $f/f_0$ , is a parameter which depends on conformation and molecular expansion through hydration effects [56]. It can be measured experimentally from the hydrodynamic radius (or translational diffusion coefficient) and weight-average molecular weight:

$$\frac{f}{f_0} = r_H \left( \frac{4\pi N_A}{3\bar{v}M_w} \right)^{\frac{1}{3}} \quad (2)$$

where  $N_A$  is Avogadro's number,  $f$  is the friction coefficient of the molecule and  $f_0$  is the friction coefficient for a spherical particle of the same mass and (anhydrous) volume [56]. Again, other than at pH 1, there is a minor change in the values of the frictional ratio.

#### 3.3.3. Estimation of Persistence Length

The flexibility of heparin chains can also be estimated by using the persistence length,  $L_p$  [57], where longer persistence lengths are consistent with greater chain rigidity. This was calculated using the HYDFIT program [58], and the degree of sulphate loss enabled the mass per unit length (essentially the molar mass of one nm of a polymer chain) to be fixed. The program then estimated the expected intrinsic viscosity for a given molecular weight and mass per unit length and compared this to the experimentally determined value. Again, other than at pH 1, there was little change in the persistence length. Furthermore, there is also a semiquantitative relationship between  $L_p/M_L$  and conformation [59], at least in the case of pectins, and the transition from a rigid rod to a more flexible coil occurs at  $\sim 0.01 \text{ nm}^2 \text{ mol g}^{-1}$ . Therefore, other than pH 1, the heparin samples have a relatively rigid conformation, but at pH 1, the conformation is more flexible, which is consistent with the Kuhn–Sakurada (MHKS) exponent and the translational frictional ratio.

### 3.4. Activity Change in Light of Hydrodynamic Data

The conformational data and antifactor Xa activity changes are summarised in Table 3. Persistence length ( $L_p$ ), Mark–Houwink exponent ( $a$ ) and frictional ratio ( $f/f_0$ ) show minor changes, except for the sample hydrolysed pH 1/48 h/80 °C. For this sample, the most substantial antifactor Xa activity loss was observed. In previous studies, Stivala et al. (1967) linked the decrease in frictional parameters with activity loss [60], confirmed in the following analysis by Erlich and Stivala (1974) [61]. However, pH 1 was also associated with the most substantial desulphation (Table 2). The activity drop was detected for only two more samples that were also desulphated, i.e., pH 3 and pH 12 (Table 2). Considering the previously demonstrated effect of desulphation on the anticoagulation activity of heparin [8,16,18] and the minor conformational changes observed here, it is hard to draw unambiguous conclusions regarding the exclusive influence of the latter. Preferably, both

(desulphation and conformational changes) should be considered in parallel, suggesting the ‘driving force’, where appropriate. For example, the desulphation of heparin was the most probable driving force affecting the activity of heparin when exposed to milder acidic conditions (pH 3, Table 2), as the conformational changes were negligible (Table 3). Nevertheless, it is useful to consider these two features, i.e., degree of desulphation and chain conformational, when investigating heparin activity, recalling that the latter is usually a consequence of the former (desulphation → conformational changes).

#### 4. Conclusions

In summary, the mild buffering conditions affected the sulphation pattern along the heparin chain. The loss of sulphate resulted in a decrease in molecular weight, which was more severe at pH 1, when the depolymerisation of the macromolecular chain also contributed to molecular weight loss. The intrinsic viscosity and sedimentation coefficient decreased proportionally to molecular weight, indicating that there were few or no conformational changes other than at pH 1. This trend was confirmed by physical parameters: the persistence length ( $L_p$ ); the ratio of the persistence length to the mass per unit length ( $L_p/M_L$ ); Mark–Houwink exponent ( $a$ ) and frictional ratio ( $f/f_0$ ), which were similar under all conditions other than pH 1. The collected results were analysed concerning the antifactor Xa activity of pharmacological heparin, changes which probably arose due to de-N-sulphation. This study demonstrates that it is essential to carefully evaluate the conditions applied in the treatment, processing and storing of heparin designated for medical use.

**Author Contributions:** Conceptualization, G.A.M. and A.M.K.; methodology, A.M.K.; formal analysis, A.M.K., G.A.M., V.D., T.M. and J.P.R.; investigation, A.M.K.; resources, S.E.H. and G.A.M.; writing—original draft preparation, A.M.K.; writing—review and editing, S.E.H., A.M.S., E.A.Y., J.P.R. and G.A.M.; visualization, A.M.K.; supervision, G.A.M.; funding acquisition, A.M.S. and G.A.M. All authors have read and agreed to the published version of the manuscript.

**Funding:** This research received no external funding.

**Institutional Review Board Statement:** Not applicable.

**Data Availability Statement:** Available upon request.

**Acknowledgments:** The authors would like to thank LEO Pharma A/S (Ballerup, Denmark) for the heparin samples and for helping with pharmacological activity analysis.

**Conflicts of Interest:** The authors declare no conflict of interest.

#### References

1. Mulloy, B.; Khan, S.; Perkins, S.J. Molecular Architecture of Heparin and Heparan Sulfate: Recent Developments in Solution Structural Studies. *Pure Appl. Chem.* **2012**, *84*, 65–76. [[CrossRef](#)]
2. Mulloy, B. Heparin—A Century of Progress. In *Handbook of Experimental Pharmacology*; Lever, R., Mulloy, B., Page, C.P., Eds.; Springer: Berlin/Heidelberg, Germany, 2012; Volume 207, ISBN 978-3-642-23055-4.
3. Linhardt, R.J.; Claude, S. Hudson Award Address in Carbohydrate Chemistry. Heparin: Structure and Activity. *J. Med. Chem.* **2003**, *46*, 2551–2564. [[CrossRef](#)] [[PubMed](#)]
4. Bhaskar, U.; Sterner, E.; Hickey, A.M.; Onishi, A.; Zhang, F.; Dordick, J.S.; Linhardt, R.J. Engineering of Routes to Heparin and Related Polysaccharides. *Appl. Microbiol. Biotechnol.* **2012**, *93*, 1–16. [[CrossRef](#)]
5. Rudd, T.R.; Yates, E.A. A Highly Efficient Tree Structure for the Biosynthesis of Heparan Sulfate Accounts for the Commonly Observed Disaccharides and Suggests a Mechanism for Domain Synthesis. *Mol. Biosyst.* **2012**, *8*, 1499–1506. [[CrossRef](#)] [[PubMed](#)]
6. Rabenstein, D.L. Heparin and Heparan Sulfate: Structure and Function. *Nat. Prod. Rep.* **2002**, *19*, 312–331. [[CrossRef](#)] [[PubMed](#)]
7. Rubinson, K.A.; Chen, Y.; Cress, B.F.; Zhang, F.; Linhardt, R.J. Heparin’s Solution Structure Determined by Small-Angle Neutron Scattering. *Biopolymers* **2016**, *105*, 905–913. [[CrossRef](#)]
8. Skidmore, M.; Guimond, S.; Rudd, T.; Fernig, D.; Turnbull, J.; Yates, E. The Activities of Heparan Sulfate and Its Analogue Heparin Are Dictated by Biosynthesis, Sequence, and Conformation. *Connect. Tissue Res.* **2008**, *49*, 140–144. [[CrossRef](#)] [[PubMed](#)]
9. Palhares, L.C.G.F.; London, J.A.; Kozłowski, A.M.; Esposito, E.; Chavante, S.F.; Ni, M.; Yates, E.A. Chemical Modification of Glycosaminoglycan Polysaccharides. *Molecules* **2021**, *26*, 5211. [[CrossRef](#)]
10. Capila, I.; Linhardt, R.J. Heparin-Protein Interactions. *Angew. Chemie Int. Ed.* **2002**, *41*, 390–412. [[CrossRef](#)]

11. Pomin, V.H. NMR Chemical Shifts in Structural Biology of Glycosaminoglycans. *Anal. Chem.* **2014**, *86*, 65–94. [[CrossRef](#)]
12. Yates, E.A.; Gallagher, J.T.; Guerrini, M. Introduction to the Molecules Special Edition Entitled 'Heparan Sulfate and Heparin: Challenges and Controversies': Some Outstanding Questions in Heparan Sulfate and Heparin Research. *Molecules* **2019**, *24*, 1399. [[CrossRef](#)]
13. Onishi, A.; Ange, K.S.; Dordick, J.S.; Linhardt, R.J. Heparin and Anticoagulation. *Front. Biosci.* **2016**, *21*, 1372–1392. [[CrossRef](#)]
14. Jaffer, I.H.; Weitz, J.I. Antithrombotic Therapy. In *Rutherford's Vascular Surgery*; Cronenwett, J.L., Wayne Johnston, K., Eds.; Saunders Elsevier: Philadelphia, PA, USA, 2014; pp. 549–566. ISBN 9781455753048.
15. Lundin, L.; Larsson, H.; Kreuger, J.; Kanda, S.; Lindahl, U.; Salmivirta, M.; Claesson-Welsh, L. Selectively Desulfated Heparin Inhibits Fibroblast Growth Factor-Induced Mitogenicity and Angiogenesis. *J. Biol. Chem.* **2000**, *275*, 24653–24660. [[CrossRef](#)]
16. Mulloy, B.; Hogwood, J.; Gray, E.; Lever, R.; Page, C.P. Pharmacology of Heparin and Related Drugs. *Pharmacol. Rev.* **2015**, *68*, 76–141. [[CrossRef](#)] [[PubMed](#)]
17. Sugaya, N.; Habuchi, H.; Nagai, N.; Ashikari-Hada, S.; Kimata, K. 6-O-Sulfation of Heparan Sulfate Differentially Regulates Various Fibroblast Growth Factor-Dependent Signalings in Culture. *J. Biol. Chem.* **2008**, *283*, 10366–10376. [[CrossRef](#)]
18. Jorpes, E.; Bergström, S. On the Relationship between the Sulphur Content and the Anticoagulant Activity of Heparin Preparations. *Biochem. J.* **1939**, *33*, 47–52. [[CrossRef](#)]
19. Mulloy, B.; Forster, M.J.; Jones, C.; Davies, D.B. N.m.r. and Molecular-Modelling Studies of the Solution Conformation of Heparin. *Biochem. J.* **1993**, *293*, 849–858. [[CrossRef](#)]
20. Casu, B.; Naggi, A.; Torri, G. Re-Visiting the Structure of Heparin. *Carbohydr. Res.* **2015**, *403*, 60–68. [[CrossRef](#)]
21. Sun, S.F. *Physical Chemistry of Macromolecules: Basic Principles and Issues*, 2nd ed.; John Wiley & Sons: Hoboken, NJ, USA, 2004; ISBN 9786468600.
22. Cui, S.W. *Food Carbohydrates: Chemistry, Physical Properties, and Applications*, 1st ed.; Taylor & Francis: Boca Raton, FL, USA, 2005; ISBN 9780849315749.
23. Finch, P. *Carbohydrates Structures, Syntheses and Dynamics*, 1st ed.; Springer Science & Business Media: London, UK, 1999; ISBN 9789048140336.
24. Ferro, D.R.; Provasoli, A.; Ragazzi, M.; Torri, G.; Casu, B.; Gatti, G.; Jacquinet, J.C.; Sinay, P.; Petitou, M.; Choay, J. Evidence for Conformational Equilibrium of the Sulfated L-Iduronate Residue in Heparin and in Synthetic Heparin Mono- and Oligo-Saccharides: NMR and Force-Field Studies. *J. Am. Chem. Soc.* **1986**, *108*, 6773–6778. [[CrossRef](#)]
25. Hricovíni, M. Solution Structure of Heparin Pentasaccharide: NMR and DFT Analysis. *J. Phys. Chem. B* **2015**, *119*, 12397–12409. [[CrossRef](#)] [[PubMed](#)]
26. Mulloy, B.; Forster, M.J. Conformation and Dynamics of Heparin and Heparan Sulfate. *Glycobiology* **2000**, *10*, 1147–1156. [[CrossRef](#)] [[PubMed](#)]
27. Hsieh, P.H.; Thieker, D.F.; Guerrini, M.; Woods, R.J.; Liu, J. Uncovering the Relationship between Sulphation Patterns and Conformation of Iduronic Acid in Heparan Sulphate. *Sci. Rep.* **2016**, *6*, 29602. [[CrossRef](#)] [[PubMed](#)]
28. Pomin, V.H. Solution NMR Conformation of Glycosaminoglycans. *Prog. Biophys. Mol. Biol.* **2014**, *114*, 61–68. [[CrossRef](#)] [[PubMed](#)]
29. Gray, E.; Mulloy, B.; Barrowcliffe, T.W. Heparin and Low-Molecular-Weight Heparin. *Thromb. Haemost.* **2008**, *99*, 807–818. [[CrossRef](#)] [[PubMed](#)]
30. Sufliata, M.; Fu, L.; He, W.; Koffas, M.; Linhardt, R.J. Heparin and Related Polysaccharides: Synthesis Using Recombinant Enzymes and Metabolic Engineering. *Appl. Microbiol. Biotechnol.* **2015**, *99*, 7465–7479. [[CrossRef](#)] [[PubMed](#)]
31. Linhardt, R. Chemical and Enzymatic Methods for the Depolymerization and Modification of Heparin. In *Carbohydrates: Synthetic Methods and Applications in Medicinal Chemistry*; Suami, T., Ogura, H., Hasegawa, A., Eds.; VCH Publishers: Cambridge, UK, 1992; pp. 385–401. ISBN 1-56081-701-1.
32. Khan, S.; Fung, K.W.; Rodriguez, E.; Patel, R.; Gor, J.; Mulloy, B.; Perkins, S.J. The Solution Structure of Heparan Sulfate Differs from That of Heparin: Implications for Function. *J. Biol. Chem.* **2013**, *288*, 27737–27751. [[CrossRef](#)]
33. Nunes, Q.M.; Su, D.; Brownridge, P.J.; Simpson, D.M.; Sun, C.; Li, Y.; Bui, T.P.; Zhang, X.; Huang, W.; Rigden, D.J.; et al. The Heparin-Binding Proteome in Normal Pancreas and Murine Experimental Acute Pancreatitis. *PLoS ONE* **2019**, *14*, e0217633. [[CrossRef](#)]
34. Kozłowski, A.M.; Yates, E.A.; Roubroeks, J.P.; Tømmeraas, K.; Smith, A.M.; Morris, G.A. Hydrolytic Degradation of Heparin in Acidic Environments: Nuclear Magnetic Resonance Reveals Details of Selective Desulfation. *ACS Appl. Mater. Interfaces* **2021**, *13*, 5551–5563. [[CrossRef](#)]
35. Bedini, E.; Laezza, A.; Parrilli, M.; Iadonisi, A. A Review of Chemical Methods for the Selective Sulfation and Desulfation of Polysaccharides. *Carbohydr. Polym.* **2017**, *174*, 1224–1239. [[CrossRef](#)]
36. Harding, S.E.; Tombs, M.P.; Adams, G.G.; Paulsen, B.S.; Inngjerdigen, K.T.; Barsett, H. *An Introduction to Polysaccharide Biotechnology*, 2nd ed.; CRC Press: Boca Raton, FL, USA, 2017; Volume 80, ISBN 9781315372730.
37. Van Der Meer, J.Y.; Kellenbach, E.; Van Den Bos, L.J. From Farm to Pharma: An Overview of Industrial Heparin Manufacturing Methods. *Molecules* **2017**, *22*, 1025. [[CrossRef](#)]
38. Racine, E. Differentiation of the Low-Molecular-Weight Heparins. *Pharmacotherapy* **2001**, *21*, 62S–70S. [[CrossRef](#)]
39. Bienkowski, M.J.; Conrad, H.E. Structural Characterization of the Oligosaccharides Formed by Depolymerization of Heparin with Nitrous Acid. *J. Biol. Chem.* **1985**, *260*, 356–365. [[CrossRef](#)] [[PubMed](#)]

40. Kozłowski, A.M.; Yates, E.A.; Roubroeks, J.P.; Tømmeraas, K.; Larsen, F.H.; Smith, A.M.; Morris, G.A. Monitoring the Stability of Heparin: NMR Evidence for the Rearrangement of Sulfated Iduronate in Phosphate Buffer. *Carbohydr. Polym.* **2023**, *308*, 120649. [[CrossRef](#)] [[PubMed](#)]
41. Wojtasz-Mucha, J. *Pre-Extraction of Wood Components. Mild Hydrothermal Methods for a Future Materials Biorefinery*; Chalmers University of Technology: Gothenburg, Sweden, 2020.
42. Rej, R.N.; Perlin, A.S. Base-Catalyzed Conversion of the  $\alpha$ -l-Iduronic Acid 2-Sulfate Unit of Heparin into a Unit of  $\alpha$ -l-Galacturonic Acid, and Related Reactions. *Carbohydr. Res.* **1990**, *200*, 437–447. [[CrossRef](#)]
43. Danishefsky, I.; Eiber, H.B.; Carr, J.J. Investigations on the Chemistry of Heparin. I. Desulfation and Acetylation. *Arch. Biochem. Biophys.* **1960**, *90*, 114–121. [[CrossRef](#)] [[PubMed](#)]
44. Jandik, K.A.; Kruep, D.; Cartier, M.; Linhardt, R.J. Accelerated Stability Studies of Heparin. *J. Pharm. Sci.* **1996**, *85*, 45–51. [[CrossRef](#)]
45. Mohan, C. *Buffers. A Guide for the Preparation and Use of Buffers in Biological Systems*, 3rd ed.; EMD Bioscience: San Diego, CA, USA, 2006.
46. Preparation of Buffer Solutions. Available online: <http://delloyd.50megs.com/moreinfo/buffers2.html> (accessed on 3 April 2020).
47. Mulloy, B.; Heath, A.; Shriver, Z.; Jameison, F.; Al Hakim, A.; Morris, T.S.; Szajek, A.Y. USP Compendial Methods for Analysis of Heparin: Chromatographic Determination of Molecular Weight Distributions for Heparin Sodium. *Anal. Bioanal. Chem.* **2014**, *406*, 4815–4823. [[CrossRef](#)]
48. Theisen, A.; Deacon, M.P.; Johann, C.; Harding, S. *Refractive Increment Data-Book: For Polymer and Biomolecular Scientists*, 1st ed.; Nottingham University Press: Nottingham, UK, 2000.
49. Harding, S.E. Analysis of Polysaccharides by Ultracentrifugation. Size, Conformation and Interactions in Solution. In *Polysaccharides I*; Springer: Berlin/Heidelberg, Germany, 2005; Volume 186, pp. 211–254. ISBN 3-540-26112-5.
50. Schuck, P. Sedimentation Analysis of Noninteracting and Self-Associating Solutes Using Numerical Solutions to the Lamm Equation. *Biophys. J.* **1998**, *75*, 1503–1512. [[CrossRef](#)]
51. Morris, G.A.; Castile, J.; Smith, A.; Adams, G.G.; Harding, S.E. The Kinetics of Chitosan Depolymerisation at Different Temperatures. *Polym. Degrad. Stab.* **2009**, *94*, 1344–1348. [[CrossRef](#)]
52. Morris, G.A.; Adams, G.G.; Harding, S.E. On Hydrodynamic Methods for the Analysis of the Sizes and Shapes of Polysaccharides in Dilute Solution: A Short Review. *Food Hydrocoll.* **2014**, *42*, 318–334. [[CrossRef](#)]
53. Kozłowski, A.M. *Study of Hydrolytic Degradation of Heparin in Acidic and Alkaline Environments*; University of Huddersfield: Huddersfield, UK, 2021.
54. Pavlov, G.; Finet, S.; Tatarenko, K.; Korneeva, E.; Ebel, C. Conformation of Heparin Studied with Macromolecular Hydrodynamic Methods and X-Ray Scattering. *Eur. Biophys. J.* **2003**, *32*, 437–449. [[CrossRef](#)]
55. Morris, G.A.; Foster, T.J.; Harding, S.E. A Hydrodynamic Study of the Depolymerisation of a High Methoxy Pectin at Elevated Temperatures. *Carbohydr. Polym.* **2002**, *48*, 361–367. [[CrossRef](#)]
56. Tanford, C. *Physical Chemistry of Macromolecules*; Gaylord, N.G., Gibbs, J.H., Eds.; John Wiley & Sons: New York, NY, USA, 1961.
57. Harding, S.E. The Intrinsic Viscosity of Biological Macromolecules. Progress in Measurement, Interpretation and Application to Structure in Dilute Solution. *Prog. Biophys. Mol. Biol.* **1997**, *68*, 207–262. [[CrossRef](#)] [[PubMed](#)]
58. Ortega, A.; García de la Torre, J. Equivalent Radii and Ratios of Radii from Solution Properties as Indicators of Macromolecular Conformation, Shape, and Flexibility. *Biomacromolecules* **2007**, *8*, 2464–2475. [[CrossRef](#)]
59. Morris, G.A.; Ralet, M.-C. The Effect of Neutral Sugar Distribution on the Dilute Solution Conformation of Sugar Beet Pectin. *Carbohydr. Polym.* **2012**, *88*, 1488–1491. [[CrossRef](#)]
60. Stivala, S.S.; Yuan, L.; Ehrlich, J.; Liberti, P.A. Physicochemical Studies of Fractionated Bovine Heparin. III. Some Physical Parameters in Relation to Biological Activity. *Arch. Biochem. Biophys.* **1967**, *122*, 32–39. [[CrossRef](#)] [[PubMed](#)]
61. Ehrlich, J.; Stivala, S.S. Macromolecular Properties of Heparin in Dilute Solution: 2. Dimensional Parameters as a Function of PH, Ionic Strength and Desulphation. *Polymer* **1974**, *15*, 204–210. [[CrossRef](#)]

**Disclaimer/Publisher's Note:** The statements, opinions and data contained in all publications are solely those of the individual author(s) and contributor(s) and not of MDPI and/or the editor(s). MDPI and/or the editor(s) disclaim responsibility for any injury to people or property resulting from any ideas, methods, instructions or products referred to in the content.